

Interfering pathways for photon blockade in cavity QED with one and two qubits

K. Hou,^{1,2} C. J. Zhu,^{1,*} Y. P. Yang,^{1,†} and G. S. Agarwal^{3,‡}

¹*MOE Key Laboratory of Advanced Micro-Structured Materials,*

School of Physics Science and Engineering, Tongji University, Shanghai, China 200092

²*Department of Mathematics and Physics, Anhui JianZhu University, Hefei 230601, China*

³*Institute for Quantum Science and Engineering,*

and Department of Biological and Agricultural Engineering Texas A&M University, College Station, Texas 77843, USA

We theoretically study the quantum interference induced photon blockade phenomenon in atom cavity QED system, where the destructive interference between two different transition pathways prohibits the two-photon excitation. Here, we first explore the single atom cavity QED system via an atom or cavity drive. We show that the cavity-driven case will lead to the quantum interference induced photon blockade under a specific condition, but the atom driven case can't result in such interference induced photon blockade. Then, we investigate the two atoms case, and find that an additional transition pathway appears in the atom-driven case. We show that this additional transition pathway results in the quantum interference induced photon blockade only if the atomic resonant frequency is different from the cavity mode frequency. Moreover, in this case, the condition for realizing the interference induced photon blockade is independent of the system's intrinsic parameters, which can be used to generate antibunched photon source both in weak and strong coupling regimes.

I. INTRODUCTION

The phenomenon of quantum interference (QI) effect [1] occurs between different photon transmission pathways, leading to the inhibition/attenuation of absorption by the destructive interference [2]. With its fascinating physical mechanism, many novel quantum effects and corresponding applications have emerged, e.g., electromagnetically induced transparency (EIT) [3], coherent population trapping (CPT) [4], laser without inversion [5], light with ultraslow group velocity [6] and so on. Specifically, quantum interference between two photons has been observed in experiments [7, 8]. Moreover, the QI effect can result in a new type of photon blockade (PB) phenomenon in cavity QED systems [9].

The traditional PB results from the anharmonicity of the Jaynes Cummings ladder in atom cavity QED systems [10], where the absorption of the first photon blocks the transmission of the second photon. As a result, one can observe an orderly output of photons one by one with strong photon antibunching and the sub-Poissonian statistics. Up to now, the traditional PB has been experimentally demonstrated in various quantum systems, including atoms [11, 12], quantum dot [13] and ions cavity quantum electrodynamics systems [14] as well as the circuit-QED systems [15, 16].

To blockade the transmission of the second photon, strong coupling limit is required in the traditional PB, which is challenging in experiments, especially for semiconductor cavity QED systems. In addition, with current experimental techniques, the second order correlation function $g^{(2)}$, which is a signature for PB, can't

be close to zero to achieve perfect antibunched photons. This is because the two-photon and multiphoton excitations cannot be inhibited due to the energy broadening. In the light of these disadvantages, a novel physical mechanism based on quantum interference is proposed to generate strong PB phenomenon [17]. In literature, this quantum interference induced PB is known as the unconventional photon blockade (UPB). In general, there exist two methods to open an additional transition pathway for generating the quantum interference effect. One is by adding an auxiliary cavity with the coherent mode coupling [17–19], while the other is by adding an auxiliary driving field [20, 21].

To date, the UPB has been theoretically investigated in various systems, such as two tunnel-coupled cavity system [22–26], quantum dots [27–29], quantum well [22], nanomechanical resonator [30], optomechanical system [31, 32], optical parametric amplifier system [33], as well as the hybrid quantum plasmonic system [34]. Recently, the UPB is experimentally demonstrated in two coupled superconducting resonators [35] and a single quantum dot cavity QED system driven by two orthogonally polarized modes [36].

In this paper, we theoretically investigate the quantum interference induced photon blockade in atom cavity QED systems via an atom or cavity drive. Using the amplitude method, we obtain the condition for observing the interference induced photon blockade in the atom cavity QED system via a cavity drive, i.e., equation (5). To the best of our knowledge, this condition has not yet been reported in the literature. Opposite to the work in Ref. [9], we show that the interference induced photon blockade can be realized without requiring the weak non-linearity or auxiliary pumping field. Moreover, we show that additional transition pathways take place by adding another atom in the cavity. These additional transition pathways result in the interference induced photon block-

* Corresponding author: cjzhu@tongji.edu.cn

† Corresponding author: yang_yaping@tongji.edu.cn

‡ Corresponding author: girish.agarwal@tamu.edu

ade even via an atom drive. Therefore, extremely strong antibunching photons can be accomplished, leading to the value of the second-order correlation function smaller than unity.

The paper is arranged as follows. In section II, we first study the single atom case via a cavity drive or an atom drive. We show that the destructive interference can only be observed in the case of the cavity drive because the destructive interference can be achieved between transition pathways with odd number of photons. However, there is no interference in the case of the atom drive. This is contrary to intuition as one generally views that atom drive and cavity drive should be similar physics. In section III, we study the two atoms case also via a cavity drive or an atom drive. We show that the odd-photon transition induced destructive interference in cavity driven case can be improved by the collective coupling enhancement, leading to a significant improvement of the photon blockade phenomenon. In the atom-driven case, surprisingly, we find that an additional transition pathway appears in the presence of the second atom, yielding interference between transitions with even number of photons. If the atomic resonant frequency is the same as the cavity mode frequency, we show that this interference is constructive, so that the photon blockade can not be observed. In section IV, we show that this even-photon interference can be destructive when the atomic resonant frequency is not the same as the cavity mode frequency. As a result, two transition pathways become distinguishable, leading to the interference induced photon blockade. We also show that the condition for realizing this even-photon interference induced PB in atom-driven scheme is insensitive to the atom-cavity coupling strength. Thus, one can increase the coupling strength to obtain reasonable photon number with strong PB effect.

II. SINGLE ATOM CAVITY QED SYSTEM

First, we consider a typical single atom cavity QED system as shown in Fig. 1(a). In the frame rotating at the driving frequency ω_d , the system Hamiltonian is written as [37] (setting $\hbar = 1$)

$$H_1 = -\Delta_c a^\dagger a - \Delta_a \sigma^\dagger \sigma + g(\sigma a^\dagger + \sigma^\dagger a) + H_d, \quad (1)$$

where H_d is the driving term. If the cavity (atom) is driven by a coherent field, $H_d = \eta(a + a^\dagger)$ [$H_d = \eta(\sigma_j + \sigma_j^\dagger)$] with η being the driving strength. Here, $\Delta_c = \omega_d - \omega_c$ and $\Delta_a = \omega_d - \omega_a$ are the detunings for the cavity and atom, respectively. a (a^\dagger) is the annihilation (creation) operator of the cavity mode with the resonant frequency ω_c . σ (σ^\dagger) denotes the lowering (raising) operator of the two-level atom with the resonant transition frequency ω_a . g is the atom-cavity coupling strength.

The dynamics of this open quantum system is governed by the master equation, i.e.,

$$\frac{\partial \rho}{\partial t} = -i[H, \rho] + \mathcal{L}_\kappa \rho + \mathcal{L}_\gamma \rho, \quad (2)$$

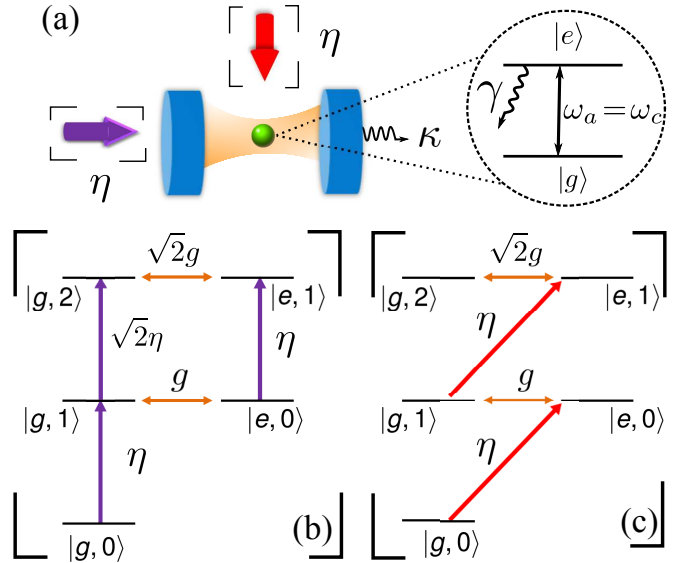


FIG. 1. (Color online) (a) Sketch of a two-level atom with resonant frequency ω_a trapped in a single-mode cavity. The red (purple) arrow corresponds to the atom (cavity) drive with driving strength η . $|g\rangle$ ($|e\rangle$) is the ground (excited) state of the atom. γ and κ are the atomic and cavity decay rates, respectively. Panels (b) and (c) show the transition pathways in an atom- and cavity-driven cases, respectively. Here yellow arrows represent the atom-cavity coupling with strength g . $|\alpha, n\rangle$ ($\alpha = g, e$) is the product state of atomic state $|\alpha\rangle$ and photon state $|n\rangle$.

where $\mathcal{L}_\kappa \rho = \kappa(2a\rho a^\dagger - a^\dagger a \rho - \rho a^\dagger a)$ and $\mathcal{L}_\gamma \rho = \gamma(2\sigma\rho\sigma^\dagger - \sigma^\dagger\sigma\rho - \rho\sigma^\dagger\sigma)$ describe the dissipations of the cavity and atom with the decay rate κ and γ , respectively. Numerically solving Eq. (2), one can obtain the second-order photon-photon correlation function $g^{(2)}(0) = \langle a^\dagger a^\dagger a a \rangle / \langle a^\dagger a \rangle^2$ in the steady state. In general, the value of $g^{(2)}(0)$ characterizes the probability of detecting two photons at the same time. If $g^{(2)}(0) > 1$, two photons will be detected simultaneously. However, if $g^{(2)}(0) < 1$, the output of photons has antibunching behavior, i.e., detecting photons one by one. In the following, we will discuss this phenomenon in detail.

Cavity-driven scheme. - We consider that the cavity is driven by a coherent field and assume $\Delta_a = \Delta_c = 0$ for simplicity. Thus, the transition pathways of this cavity-driven scheme is shown in Fig. 1(b), where $|\alpha, n\rangle$ represent the states in the atom-cavity product space. Obviously, there exist two transition pathways corresponding to the transition from $|g, 1\rangle$ to $|g, 2\rangle$. The first one is $|g, 1\rangle \xrightarrow{\sqrt{2}\eta} |g, 2\rangle$ transition, and the second one is $|g, 1\rangle \xrightarrow{g} |e, 0\rangle \xrightarrow{\eta} |e, 1\rangle \xrightarrow{\sqrt{2}g} |g, 2\rangle$ transition. If the destructive interference takes place between these two transition pathways, the two-photon excitation will be not allowed and the probability for detecting the state $|g, 2\rangle$ will be zero. Then, one can achieve quantum inter-

ference induced photon blockade phenomenon, leading to an output of antibunched photons.

To obtain the condition for this destructive interference, we assume the system wavefunction $\Psi \approx \sum_{n=0}^2 C_{g,n}|g, n\rangle + \sum_{n=0}^1 C_{e,n}|e, n\rangle$, where $|C_{\alpha,n}|^2$ ($\alpha = g, e$) is the probability for detecting the state $|\alpha, n\rangle$. Here, other states in larger photon-number spaces have been neglected since the driving field is not strong enough to excite these states. Then, the dynamical equations for the amplitudes of each state can be written as

$$i\dot{C}_{g,1} = gC_{e,0} - i\frac{\kappa}{2}C_{g,1} + \eta C_{g,0} + \sqrt{2}\eta C_{g,2}, \quad (3a)$$

$$i\dot{C}_{g,2} = \sqrt{2}gC_{e,1} - i\kappa C_{g,2} + \sqrt{2}\eta C_{g,1}, \quad (3b)$$

$$i\dot{C}_{e,0} = gC_{g,1} - i\frac{\gamma}{2}C_{e,0} + \sqrt{2}\eta C_{e,1}, \quad (3c)$$

$$i\dot{C}_{e,1} = \sqrt{2}gC_{g,2} - i\left(\frac{\kappa + \gamma}{2}\right)C_{e,1} + \eta C_{e,0}. \quad (3d)$$

Using the perturbation method [9, 38] and solving above equations under the steady state approximation, one can obtain

$$C_{g,2} = \frac{2\sqrt{2}\eta^2(-\gamma^2 - \gamma\kappa + 4g^2 - 4\eta^2)}{(\gamma\kappa + 4g^2)(\gamma\kappa + 4g^2 + \kappa^2) + 4\eta^2 X}, \quad (4)$$

with $X = 4\eta^2 - 8g^2 + \gamma^2 + \kappa^2 + \gamma\kappa$. Clearly, the optimal condition for $C_{g,2} = 0$ is

$$g = \frac{1}{2}\sqrt{\gamma^2 + \gamma\kappa + 4\eta^2}. \quad (5)$$

Under the weak driving condition, the second-order correlation function can be expressed as $g^{(2)}(0) \approx 2|C_{g,2}|^2/|C_{g,1}|^4$, yielding $g^{(2)}(0) \rightarrow 0$ if Eq. (5) is satisfied.

It is worth to point out that Eq. (5) is the condition for achieving destructive interference induced photon blockade in a single atom cavity QED system, as far as we known, which has not yet been reported before. Compared with the works in Refs. [35, 36, 38], our system is much simpler than their proposals, where the destructive interference results from the transition pathways between two cavity modes and weak nonlinearity is essential to realize the destructive interference. Eq. (5) implies that, under weak atom cavity coupling, the photon blockade can also be accomplished in a typical single atom cavity QED system via the destructive interference. It is noted that Eq. (5) is only valid for the weak driving field since high-order photon states are assumed to be unexcited. For strong driving field, however, Eq. (5) is invalid and one can not observe the interference induced photon blockade since high-order photon states will be excited, yielding $g^{(2)}$ larger than unity.

To verify the above analysis, we numerically solve Eq. (2). In Fig. 2(a), we plot the equal-time second-order correlation function $g^{(2)}(0)$ as a function of atom-cavity coupling strength with atomic decay rate $\gamma = \kappa$ (blue dashed curve) and $\gamma = \kappa/2$ (red solid curve), respectively. Other system parameters are given by $\Delta_a = \Delta_c = 0$

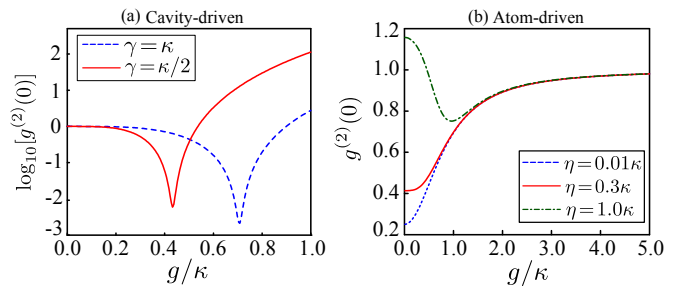


FIG. 2. (Color online) The equal-time second-order correlation function $g^{(2)}(0)$ versus the normalized coupling strength g/κ in the (a) cavity-driven and (b) atom-driven systems, respectively. In panel (a), we choose $\gamma = \kappa$ (blue dashed curve) and $\gamma = \kappa/2$ (red solid curve), respectively. The driving strength $\eta = 0.01\kappa$. In panel (b), we choose $\gamma = \kappa$, but the driving strength is chosen as $\eta = 0.01\kappa$ (blue dashed curve), $\eta = 0.3\kappa$ (red solid curve) and $\eta = \kappa$ (green dash dotted curve), respectively.

and $\eta = 0.01\kappa$. It is clear to see that there exist a minimum in the second-order correlation function at $g = \sqrt{\gamma(\gamma + \kappa) + 4\eta^2}/2$ due to the destructive interference effect. Moreover, the smaller the atomic decay rate is, the smaller the value of $g^{(2)}(0)$ is, leading to a stronger photon blockade effect as shown in Fig. 2(a).

No quantum interference for atom-driven scheme. - Contrary to the cavity-driven case, there exists only one transition pathway for the two-photon excitation, i.e., $|g, 0\rangle \xrightarrow{\eta} |e, 0\rangle \xrightarrow{g} |g, 1\rangle \xrightarrow{\eta} |e, 1\rangle \xrightarrow{\sqrt{2}g} |g, 2\rangle$ [see Fig. 1(c)] if one drive the atom directly. Therefore, the two-photon excitations can't be blocked by the quantum interference effect. In the case of weak driving strength, e.g., $\eta = 0.01\kappa$ (blue dashed curve) and $\eta = 0.3\kappa$ (red solid curve), the value of $g^{(2)}(0)$ is smaller than unity for small coupling strengths because the high-order states can't be excited by such weak driving fields. With the increase of the atom-cavity coupling strength, the energy splitting become dominant so that the driving field becomes far off-resonant to all states in the system, yielding $g^{(2)}(0) \rightarrow 1$ as shown in Fig. 2(b). However, in the case of strong driving strength, e.g., $\eta = \kappa$ (green dash dotted curve), states in two-photon space will be excited and one can obtain $g^{(2)}(0) > 1$ for small coupling strength g . As g increases, it is clear to see that $g^{(2)}(0) < 1$ because the anharmonic energy splitting prevents the states in two-photon space from being excited [see the green curve in Fig. 2(b)]. Furthering increasing g , one can also observe $g^{(2)}(0) \rightarrow 1$ since the driving field is in far off-resonant state.

III. TWO ATOMS CAVITY QED SYSTEM

Next, we consider that two identical atoms are trapped in a single-mode cavity with the same atom-cavity cou-

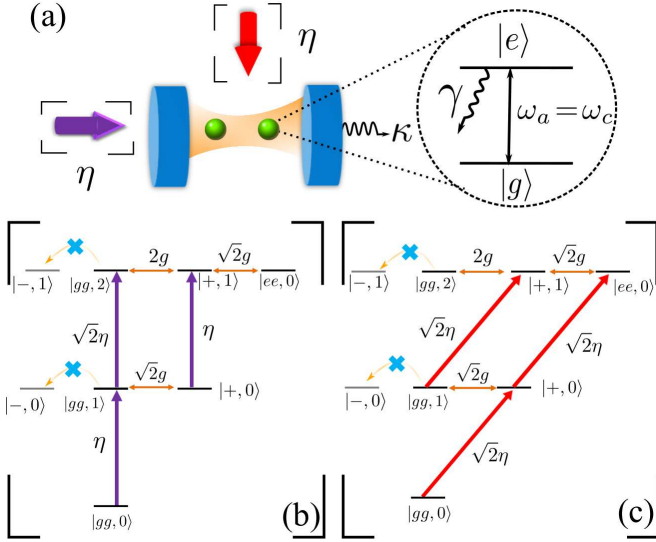


FIG. 3. (Color online) (a) Sketch of two two-level atoms trapped in a single-mode cavity. The red (purple) arrow corresponds to the atom (cavity) drive with driving strength η . Panels (b) and (c) show the transition pathways in cavity- and atom-driven systems, respectively.

pling strengths as shown in Fig. 3(a). The corresponding Hamiltonian is then written as

$$H_2 = -\Delta_c a^\dagger a + \sum_{j=1}^2 [-\Delta_a \sigma_j^\dagger \sigma_j + g(\sigma_j a^\dagger + \sigma_j^\dagger a)] + H_d, \quad (6)$$

where the subscript j indicates the j -th atom. Likewise, the drive term is given by $H_d = \eta(a^\dagger + a)$ for the cavity drive, and $H_d = \eta \sum_{j=1}^2 (\sigma_j + \sigma_j^\dagger)$ for the atom drive, respectively. Then, the master equation describing the dynamics of the system is written as

$$\frac{\partial \rho}{\partial t} = -i[H_2, \rho] + \mathcal{L}_\kappa \rho + \sum_{j=1}^2 \mathcal{L}_\gamma^{(j)} \rho, \quad (7)$$

where $\mathcal{L}_\gamma^{(j)} \rho$ represents the dissipation term of the j -th atom.

For mathematical simplicity, we assume $\Delta_a = \Delta_c = 0$. In general, such system can be described by using the collective states $\{|gg\rangle, |\pm\rangle, |ee\rangle\}$ as the basis. Here, we define the states $|\pm\rangle = (|eg\rangle \pm |ge\rangle)/\sqrt{2}$ as the symmetric and anti-symmetric Dicke states, respectively.

Cavity-driven scheme. - Since two atoms have the same coupling strength (i.e., in-phase radiation), the anti-symmetric Dicke states $|-, n\rangle$ are dark states, decoupling to other states in this system [39, 40]. In the cavity driven scheme, therefore, one can also observe two different transition pathways for the two-photon excitations, corresponding to $|gg, 1\rangle \xrightarrow{\sqrt{2}\eta} |gg, 2\rangle$ and $|gg, 1\rangle \xrightarrow{\sqrt{2}\eta} |+, 0\rangle \xrightarrow{\sqrt{2}\eta} |+, 1\rangle \xrightarrow{\sqrt{2}g} |ee, 0\rangle \xrightarrow{2g} |gg, 2\rangle$, respectively [see Fig. 3(b)].

To obtain the optimal condition for achieving the destructive quantum interference between these two pathways, we also solve the amplitude equations [similar to Eqs. (3)] by assuming the system wavefunction $\Psi \approx \sum_{n=0}^2 C_{gg,n} |gg, n\rangle + \sum_{n=0}^1 C_{\pm,n} |\pm, n\rangle + C_{ee,0} |ee, 0\rangle$. Under the steady state approximation, the probability amplitude of state $|gg, 2\rangle$ is given by

$$C_{gg,2} \approx \frac{2\sqrt{2}\gamma\eta^2 (4g^2 - \gamma^2 - \gamma\kappa - 4\eta^2)}{(\gamma\kappa + 8g^2)(\gamma^2\kappa + \gamma\kappa^2 + 8\gamma g^2 + 4g^2\kappa)}. \quad (8)$$

Obviously, one can obtain the same optimal condition for $C_{gg,2} = 0$ as given by Eq. (5), yielding strong photon blockade effect induced by the destructive interference between these two transition pathways.

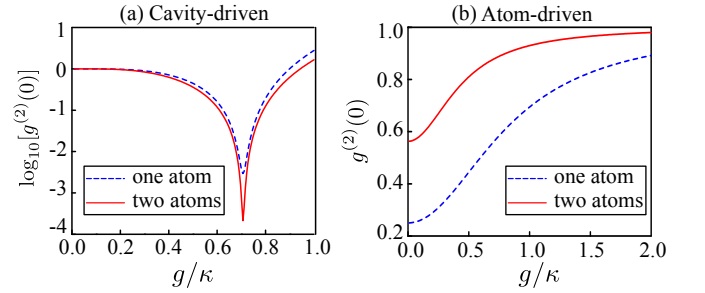


FIG. 4. (Color online) The equal-time second-order correlation function $g^{(2)}(0)$ versus the normalized coupling strength g/κ in the (a) cavity driven and (b) atom driven systems, respectively. The blue dashed curves correspond to the one atom case, while the red solid curves correspond to the two atoms case. The system parameters are given by $\Delta_a = \Delta_c = 0$, $\gamma = \kappa$ and $\eta = 0.01\kappa$, respectively.

In Fig. 4(a), we plot the equal-time second-order correlation function $g^{(2)}(0)$ as a function of the atom-cavity coupling g . The system parameters are given by $\Delta_a = \Delta_c = 0$, $\gamma = \kappa$ and $\eta = 0.01\kappa$, respectively. It is clear to see that there also exists a minimum at $g = \sqrt{\gamma(\gamma + \kappa) + 4\eta^2}/2$ for two atoms system. Compared with the single atom case, the value of $g^{(2)}(0)$ at $g = \sqrt{\gamma(\gamma + \kappa) + 4\eta^2}/2$ decreases significantly [see red curve], leading to an improvement of the photon blockade phenomenon. The physical mechanism of this PB improvement attributes to the enhanced destructive interference effect resulting from the collective coupling enhancement [see Fig. 3(b)].

Constructive quantum interference leading to no photon blockade in atom-driven scheme. - Let's consider that two atoms are driven by the coherent field. As shown in Fig. 3(c), there exist two different transition pathways for two-photon excitations, which is opposite to the single atom case. Using the same basis states, these two transition pathways can be represented by $|gg, 0\rangle \xrightarrow{\sqrt{2}\eta} |+, 0\rangle \xrightarrow{\sqrt{2}g} |gg, 1\rangle \xrightarrow{\sqrt{2}\eta} |+, 1\rangle \xrightarrow{2g} |gg, 2\rangle$ and $|+, 0\rangle \xrightarrow{\sqrt{2}\eta} |ee, 0\rangle \xrightarrow{\sqrt{2}g} |+, 1\rangle \xrightarrow{2g} |gg, 2\rangle$, respectively. To

realize the PB, the excitation of the state $|+, 1\rangle$ is required to be inhibited by the destructive interference so that the state $|gg, 2\rangle$ remains unexcited. However, these two transitions are symmetric and indistinguishable so that the interference between these two transitions are constructive [41]. Thus, the excitation of the state $|+, 1\rangle$ is allowed in this case, and can be significantly enhanced via the constructive interference. As shown in Fig. 4(b), the value of $g^{(2)}(0)$ becomes much larger than that in single atom-driven case.

IV. TWO ATOMS-DRIVEN CAVITY QED SYSTEM WITH $\omega_a \neq \omega_c$

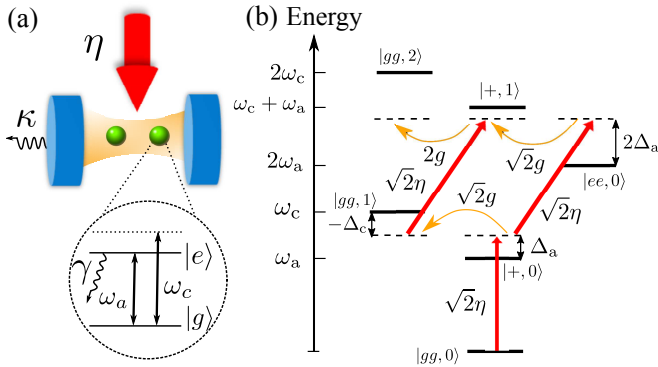


FIG. 5. (Color online) (a) Sketch of two atoms-driven cavity QED system, where two atoms are driven by a coherent field η and the atomic resonant frequency $\omega_a \neq \omega_c$. (b) The corresponding transition pathways show the destructive interference process.

Here, we also study the two atoms-driven case but $\omega_a \neq \omega_c$, i.e., the atomic and cavity resonant frequency are different [see Fig. 5(a)]. In this system, the amplitude equations are given by

$$i\dot{C}_{gg,1} = \sqrt{2}gC_{+,0} - \left(i\frac{\kappa}{2} + \Delta_c\right)C_{gg,1} + \sqrt{2}\eta C_{+,1}, \quad (9a)$$

$$i\dot{C}_{gg,2} = 2gC_{+,1} + (-2\Delta_c - i\kappa)C_{gg,2}, \quad (9b)$$

$$i\dot{C}_{+,0} = \sqrt{2}\eta C_{gg,0} - \left(\Delta_a + i\frac{\gamma}{2}\right)C_{+,0} + \sqrt{2}gC_{gg,1} + \sqrt{2}\eta C_{ee,0}, \quad (9c)$$

$$i\dot{C}_{+,1} = \sqrt{2}\eta C_{gg,1} - \left(\Delta_a + \Delta_c + i\frac{\gamma + \kappa}{2}\right)C_{+,1} + 2gC_{gg,2} + \sqrt{2}gC_{ee,0}, \quad (9d)$$

$$i\dot{C}_{ee,0} = \sqrt{2}\eta C_{+,0} - (2\Delta_a + i\gamma)C_{ee,0} + \sqrt{2}gC_{+,1}. \quad (9e)$$

Under the steady state approximation and assuming $C_{gg,0} \gg \{C_{gg,1}, C_{+,0}\} \gg \{C_{gg,2}, C_{+,1}, C_{ee,0}\}$ and

$C_{gg,0} \simeq 1$, one can obtain

$$C_{gg,2} = \frac{16\sqrt{2}g^2\eta^2[-2i(2\Delta_a + \Delta_c) + 2\gamma + \kappa]}{X(Y - 2i\Delta_a Z)}, \quad (10a)$$

$$C_{gg,1} = -\frac{8g\eta}{8g^2 - \Delta_a(4\Delta_c + 2i\kappa) - 2i\gamma\Delta_c + \gamma\kappa}, \quad (10b)$$

$$C_{+,1} = \frac{8\sqrt{2}g\eta^2(\kappa - 2i\Delta_c)[2(2\Delta_a + \Delta_c) + i(2\gamma + \kappa)]}{X(Y - 2i\Delta_a Z)}, \quad (10c)$$

where $X = \Delta_a(-4\Delta_c - 2i\kappa) - 2i\gamma\Delta_c + \gamma\kappa + 8g^2$ and $Y = -4\Delta_a^2(\kappa - 2i\Delta_c) + \gamma^2\kappa - 4\gamma\Delta_c^2 - 2i\Delta_c(\gamma^2 + 2\gamma\kappa + 4g^2) + \gamma\kappa^2 + 8\gamma g^2 + 4g^2\kappa$ and $Z = -4i\Delta_c(\gamma + \kappa) - 4\Delta_c^2 + 2\gamma\kappa + 8g^2 + \kappa^2$. Assuming $\{\Delta_a, \Delta_c\} \gg \{\gamma, \kappa\}$, the equal-time second-order correlation can be expressed as

$$g^{(2)}(0) \simeq \frac{2|C_{gg,2}|^2}{|C_{gg,1}|^4} \simeq \frac{(2\Delta_a + \Delta_c)^2(8g^2 - 4\Delta_a\Delta_c)^2}{D}, \quad (11)$$

where $D = [-8\Delta_a\Delta_c(\gamma + \kappa) - 4\kappa\Delta_a^2 + \gamma^2\kappa - 4\gamma\Delta_c^2 + \gamma\kappa^2 + 8\gamma g^2 + 4g^2\kappa]^2 + [8\Delta_a^2\Delta_c - 2\Delta_a(-4\Delta_c^2 + 2\gamma\kappa + 8g^2 + \kappa^2) - 2\Delta_c(\gamma^2 + 2\gamma\kappa + 4g^2)]^2$. Obviously, there exist two conditions to achieve $g^{(2)}(0) \rightarrow 0$, yielding an output of antibunched photons.

The first condition is $\Delta_a\Delta_c = 2g^2$, corresponding to the traditional PB. In particular, this condition can be reduced to $\Delta_a = \pm\sqrt{2}g$ if one assume $\Delta_c = \Delta_a$, which is widely known as the condition for vacuum Rabi splitting and photon blockade phenomenon in strong coupling regime [40]. It is worth to point out that the atom-cavity coupling strength must be strong enough to observe the PB at the frequencies $\Delta_a\Delta_c = 2g^2$, i.e. the strong coupling is critically important.

The second condition is $\Delta_c = -2\Delta_a$. Surprisingly, we find that it is independent to the atom-cavity coupling strength. To understand the physical mechanism of this condition, we examine these two transition pathways for two-photon excitations again. As shown in Fig. 5(b), transitions (I) $|+, 0\rangle \rightarrow |gg, 1\rangle \rightarrow |+ , 1\rangle \rightarrow |gg, 2\rangle$ and (II) $|+, 0\rangle \rightarrow |ee, 0\rangle \rightarrow |+ , 1\rangle \rightarrow |gg, 2\rangle$ are distinct as opposite to the case of $\omega_a = \omega_c$. Thus, the destructive interference will take place if this specific condition is satisfied. In general, the occupying probability of state $|+, 1\rangle$ obeys the second-order Fermi golden rule [41, 42], yielding

$$|C_{+,1}|^2 \propto \frac{\pi}{\hbar} \left| \frac{1}{\omega_a + \omega_c - 2\omega_p} + \frac{1}{\omega_a - \omega_p} \right|^2. \quad (12)$$

Clearly, the destructive interference will result in $|C_{+,1}|^2 \rightarrow 0$ if $-(\omega_a + \omega_c - 2\omega_p) = \omega_a - \omega_p$ is satisfied. As a result, there is no population in the state $|gg, 2\rangle$ and the second-order correlation function $g^{(2)}(0) \rightarrow 0$. This condition implies that the quantum interference induced PB can be implemented in two atoms-driven cavity QED system if $\omega_a \neq \omega_c$. It is worth to point out that the physical mechanism of this destructive interference between

even-photon transitions is different from that extensively studied in literature, where the interference occurs via the odd-photon transitions.

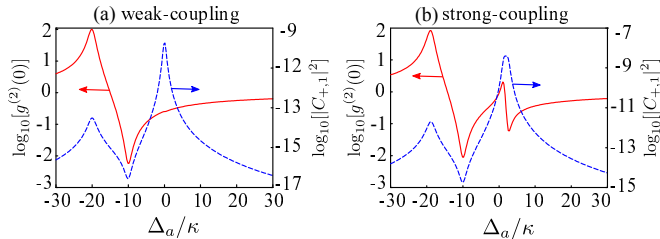


FIG. 6. (Color online) Plots of the equal-time second-order correlation function $g^{(2)}(0)$ (red solid curves) and the probability for detecting state $|C_{+,1}\rangle^2$ (blue dashed curves) as a function of the normalized detuning Δ_a/κ . Here, we choose $\gamma = \kappa$, $\Delta_c = 20\kappa$ and $\eta = 0.01\kappa$, respectively. The coupling strength is given by (a) $g = 0.5\kappa$ and (b) $g = 5\kappa$, respectively.

To verify these analytical results, we carry out numerical simulation by solving the master equation with system parameters $\Delta_c = 20\kappa$ and $\gamma = \kappa$. For weak atom-cavity coupling strength, e.g., $g = 0.5\kappa$, only a single minimum at the frequency $\Delta_a = -\Delta_c/2$ can be observed in the second-order correlation function [see Fig. 6(a), red curve]. As shown in Fig. 6(a), the value of $g^{(2)}(0)$ is smaller than 10^{-2} due to the destructive interference, resulting in a strong PB effect. Simultaneously, the value of $|C_{+,1}\rangle^2$ (blue curve) reaches its minimum, leading to $|C_{gg,2}\rangle^2 \rightarrow 0$. For strong atom-cavity coupling strength (e.g., $g = 5\kappa$), however, there exist two minima in the second-order correlation function, corresponding to the frequencies $\Delta_a = -\Delta_c/2$ and $\Delta_a = 2g^2/\Delta_c$, respectively [see Fig. 6(b), red curve]. The values for these two minima are both less than unity. The left one is resulted from the destructive interference since $|C_{gg,2}\rangle^2$ also reaches its minimum [see the blue curve], while the right one attributes to the anharmonic energy splitting. It is clear to see that the value of $g^{(2)}(0)$ at $\Delta_a = -\Delta_c/2$ is much smaller than that at $\Delta_a = 2g^2/\Delta_c$.

In Fig. 7(a), we plot the second-order correlation function $g^{(2)}(0)$ as functions of the detunings Δ_a and Δ_c , respectively. In panels (a) and (b), we chose the atom-cavity coupling strength $g = 0.5\kappa$ and $g = 5\kappa$, respectively. Other system parameters are the same as those used in Fig. (6). The dashed and dash-dotted curves indicate the analytical expressions $\Delta_a = -\Delta_c/2$ and $\Delta_a\Delta_c = 2g^2$, respectively. It is clear to see that the second order correlation function at $\Delta_a = -\Delta_c/2$ is always smaller than unity in both weak and strong coupling regimes. However, the correlation function at $\Delta_a\Delta_c = 2g^2$ is smaller than unity only when the system enters into the strong coupling regime, which matches the analytical results very well.

Finally, we discuss the influence of the atom-cavity coupling strength on the interference induced PB in this two atoms cavity QED system by setting $\Delta \equiv$

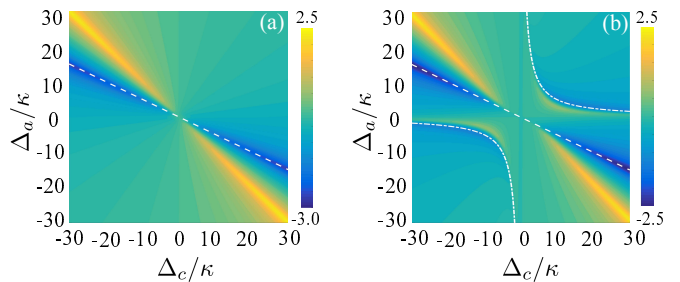


FIG. 7. (Color online) Equal-time second-order correlation function $g^{(2)}(0)$ versus the cavity detuning Δ_c and atomic detuning Δ_a , respectively. Here, the coupling strength is chosen as (a) $g = 0.5\kappa$ and (b) $g = 5\kappa$, respectively. The white dashed curves represent the traditional PB condition ($\Delta_a\Delta_c = 2g^2$) and the white dash dotted curves denote the condition of the interference induced PB ($\Delta_c = -2\Delta_a$). The other parameters are same as those used in Fig. 6.

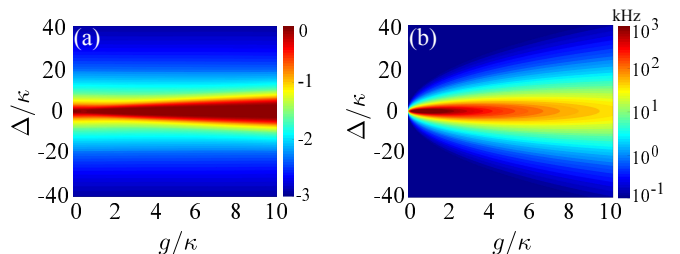


FIG. 8. (Color online) Plots of the equal-time second-order correlation function $g^{(2)}(0)$ [panel (a)] and the counting rate [panel (b)] as functions of the detuning $\Delta \equiv \Delta_a = -\Delta_c/2$ and the coupling strength g , respectively. The system parameters are chosen as $\kappa/2\pi = 2.8$ MHz, $\gamma/2\pi = 3.0$ MHz, $\eta/2\pi = 1.4$ MHz, which are the same as those given in Ref. [43].

$\Delta_a = -\Delta_c/2$. In Fig. 8(a), the second-order correlation function $g^{(2)}(0)$ is plotted as functions of the normalized atom-cavity coupling strength g/κ and the normalized detuning Δ/κ , respectively. Here, we choose a set of experimental parameters as $\kappa/2\pi = 2.8$ MHz, $\gamma/2\pi = 3.0$ MHz, $\eta/2\pi = 1.4$ MHz [43]. We notice that $g^{(2)}(0)$ decreases quickly as the detuning Δ increases, but changes slightly as the increase of the atom-cavity coupling strength g . Contrary to the second order correlation function, the counting rate of cavity photons [see panel (b)] grows significantly as the atom-cavity coupling strength g increases. Therefore, detectable photons with strong antibunching behavior can be accomplished under strong coupling regime if a specific detuning Δ is chosen.

V. CONCLUSION

In summary, we have theoretically investigated the nature of the interference induced photon blockade in cavity QED with one and two atoms. In a single atom cav-

ity QED system, we show that the interference induced photon blockade can only be observed when the external field drives the cavity directly. In the atom driven scheme, there exists a single transition pathway for the two-photon excitation so that the interference induced photon blockade cannot be observed. In two atoms cavity QED system, the quantum interference induced photon blockade still exists in cavity driven scheme. In the atom-driven case, we show that there exist two transition pathways for the two-photon excitation as opposite to the single atom case. If the atomic and cavity resonant frequencies are the same, these two transition pathways are indistinct and lead to constructive interference, which is harmful to the photon blockade effect. However, if the atomic and cavity resonant frequencies are different, these two transition pathways become distinct and lead to a new kind of photon blockade effect based on the even photon destructive interference. Moreover, we show that the condition for this novel interference in-

duced photon blockade is independent to the atom-cavity coupling strength, which provides us the possibility for observing large photon number with strong antibunching behavior in the strong coupling regime.

ACKNOWLEDGMENTS

CJZ and YPY thank the support of the National Key Basic Research Special Foundation (Grant No.2016YFA0302800); the Shanghai Science and Technology Committee (Grants No.18JC1410900); the National Nature Science Foundation (Grant No.11774262). KH thanks the support of the Natural Science Foundation of Anhui Province (Grant No.1608085QA23). Natural Science Foundation of Anhui Provincial Education Department (Grant No.KJ2018JD20). GSA thanks the support of Air Force Office of scientific Research (Award No. FA-9550-18-1-0141).

-
- [1] Z. Ficek and S. Swain, *Quantum interference and coherence: theory and experiments*, Vol. 100 (Springer Science & Business Media, 2005).
- [2] G. S. Agarwal, *Quantum optics* (Cambridge University Press, 2012, see chapters 14 and 17.).
- [3] M. Fleischhauer, A. Imamoglu, and J. P. Marangos, Electromagnetically induced transparency: Optics in coherent media, *Rev. Mod. Phys.* **77**, 633 (2005).
- [4] P. Yun, F. Tricot, C. E. Calosso, S. Micalizio, B. François, R. Boudot, S. Guérandel, and E. de Clercq, High-performance coherent population trapping clock with polarization modulation, *Phys. Rev. Applied* **7**, 014018 (2017).
- [5] M. O. Scully, S.-Y. Zhu, and A. Gavrielides, Degenerate quantum-beat laser: Lasing without inversion and inversion without lasing, *Phys. Rev. Lett.* **62**, 2813 (1989).
- [6] T. Baba, Slow light in photonic crystals, *Nat. Photonics* **2**, 465 (2008).
- [7] J. Beugnon, M. P. Jones, J. Dingjan, B. Darquié, G. Messin, A. Browaeys, and P. Grangier, Quantum interference between two single photons emitted by independently trapped atoms, *Nature* **440**, 779 (2006).
- [8] G. Araneda, D. B. Higginbottom, L. Slodička, Y. Colombe, and R. Blatt, Interference of single photons emitted by entangled atoms in free space, *Phys. Rev. Lett.* **120**, 193603 (2018).
- [9] M. Bamba, A. Imamoglu, I. Carusotto, and C. Ciuti, Origin of strong photon antibunching in weakly nonlinear photonic molecules, *Phys. Rev. A* **83**, 021802 (2011).
- [10] A. Imamoglu, H. Schmidt, G. Woods, and M. Deutsch, Strongly interacting photons in a nonlinear cavity, *Phys. Rev. Lett.* **79**, 1467 (1997).
- [11] K. M. Birnbaum, A. Boca, R. Miller, A. D. Boozer, T. E. Northup, and H. J. Kimble, Photon blockade in an optical cavity with one trapped atom, *Nature* **436**, 87 (2005).
- [12] B. Dayan, A. Parkins, T. Aoki, E. Ostby, K. Vahala, and H. Kimble, A photon turnstile dynamically regulated by one atom, *Science* **319**, 1062 (2008).
- [13] A. Faraon, I. Fushman, D. Englund, N. Stoltz, P. Petroff, and J. Vučković, Coherent generation of non-classical light on a chip via photon-induced tunnelling and blockade, *Nat. Phys.* **4**, 859 (2008).
- [14] S. Debnath, N. M. Linke, S.-T. Wang, C. Figgatt, K. A. Landsman, L.-M. Duan, and C. Monroe, Observation of hopping and blockade of bosons in a trapped ion spin chain, *Phys. Rev. Lett.* **120**, 073001 (2018).
- [15] C. Lang, D. Bozyigit, C. Eichler, L. Steffen, J. M. Fink, A. A. Abdumalikov, M. Baur, S. Filipp, M. P. da Silva, A. Blais, and A. Wallraff, Observation of resonant photon blockade at microwave frequencies using correlation function measurements, *Phys. Rev. Lett.* **106**, 243601 (2011).
- [16] A. J. Hoffman, S. J. Srinivasan, S. Schmidt, L. Spietz, J. Aumentado, H. E. Türeci, and A. A. Houck, Dispersive photon blockade in a superconducting circuit, *Phys. Rev. Lett.* **107**, 053602 (2011).
- [17] T. C. H. Liew and V. Savona, Single photons from coupled quantum modes, *Phys. Rev. Lett.* **104**, 183601 (2010).
- [18] S. Ferretti, V. Savona, and D. Gerace, Optimal antibunching in passive photonic devices based on coupled nonlinear resonators, *New J. Phys.* **15**, 025012 (2013).
- [19] X.-W. Xu and Y. Li, Strong photon antibunching of symmetric and antisymmetric modes in weakly nonlinear photonic molecules, *Phys. Rev. A* **90**, 033809 (2014).
- [20] J. Tang, W. Geng, and X. Xu, Quantum interference induced photon blockade in a coupled single quantum dot-cavity system, *Sci. Rep.* **5**, 9252 (2015).
- [21] H. Flayac and V. Savona, Unconventional photon blockade, *Phys. Rev. A* **96**, 053810 (2017).
- [22] O. Kyriienko, I. A. Shelykh, and T. C. H. Liew, Tunable single-photon emission from dipolaritons, *Phys. Rev. A* **90**, 033807 (2014).
- [23] X.-W. Xu and Y. Li, Tunable photon statistics in weakly nonlinear photonic molecules, *Phys. Rev. A* **90**, 043822 (2014).

- [24] Y. H. Zhou, H. Z. Shen, and X. X. Yi, Unconventional photon blockade with second-order nonlinearity, *Phys. Rev. A* **92**, 023838 (2015).
- [25] D. Gerace and V. Savona, Unconventional photon blockade in doubly resonant microcavities with second-order nonlinearity, *Phys. Rev. A* **89**, 031803 (2014).
- [26] H. Z. Shen, Y. H. Zhou, H. D. Liu, G. C. Wang, and X. X. Yi, Exact optimal control of photon blockade with weakly nonlinear coupled cavities, *Opt. Express* **23**, 32835 (2015).
- [27] A. Majumdar, M. Bajcsy, A. Rundquist, and J. Vučković, Loss-enabled sub-poissonian light generation in a bimodal nanocavity, *Phys. Rev. Lett.* **108**, 183601 (2012).
- [28] W. Zhang, Z. Yu, Y. Liu, and Y. Peng, Optimal photon antibunching in a quantum-dot-bimodal-cavity system, *Phys. Rev. A* **89**, 043832 (2014).
- [29] M. Cygorek, A. M. Barth, F. Ungar, A. Vagov, and V. M. Axt, Nonlinear cavity feeding and unconventional photon statistics in solid-state cavity qed revealed by many-level real-time path-integral calculations, *Phys. Rev. B* **96**, 201201 (2017).
- [30] X.-W. Xu, A.-X. Chen, and Y.-x. Liu, Phonon blockade in a nanomechanical resonator resonantly coupled to a qubit, *Phys. Rev. A* **94**, 063853 (2016).
- [31] H. Wang, X. Gu, Y.-x. Liu, A. Miranowicz, and F. Nori, Tunable photon blockade in a hybrid system consisting of an optomechanical device coupled to a two-level system, *Phys. Rev. A* **92**, 033806 (2015).
- [32] B. Sarma and A. K. Sarma, Unconventional photon blockade in three-mode optomechanics, *Phys. Rev. A* **98**, 013826 (2018).
- [33] B. Sarma and A. K. Sarma, Quantum-interference-assisted photon blockade in a cavity via parametric interactions, *Phys. Rev. A* **96**, 053827 (2017).
- [34] D. Zhao, All-optical active control of photon correlations: Dressed-state-assisted quantum interference effects, *Phys. Rev. A* **98**, 033834 (2018).
- [35] C. Vaneph, A. Morvan, G. Aiello, M. Féchant, M. Aprili, J. Gabelli, and J. Estève, Observation of the unconventional photon blockade in the microwave domain, *Phys. Rev. Lett.* **121**, 043602 (2018).
- [36] H. J. Snijders, J. A. Frey, J. Norman, H. Flayac, V. Savona, A. C. Gossard, J. E. Bowers, M. P. van Exter, D. Bouwmeester, and W. Löffler, Observation of the unconventional photon blockade, *Phys. Rev. Lett.* **121**, 043601 (2018).
- [37] C. Hamsen, K. N. Tolazzi, T. Wilk, and G. Rempe, Two-photon blockade in an atom-driven cavity qed system, *Phys. Rev. Lett.* **118**, 133604 (2017).
- [38] S. Ferretti, L. C. Andreani, H. E. Türeci, and D. Gerace, Photon correlations in a two-site nonlinear cavity system under coherent drive and dissipation, *Phys. Rev. A* **82**, 013841 (2010).
- [39] M.-O. Pleinert, J. von Zanthier, and G. S. Agarwal, Hyper-radiance from collective behavior of coherently driven atoms, *Optica* **4**, 779 (2017).
- [40] C. J. Zhu, Y. P. Yang, and G. S. Agarwal, Collective multiphoton blockade in cavity quantum electrodynamics, *Phys. Rev. A* **95**, 063842 (2017).
- [41] A. Muthukrishnan, G. S. Agarwal, and M. O. Scully, Inducing disallowed two-atom transitions with temporally entangled photons, *Phys. Rev. Lett.* **93**, 093002 (2004).
- [42] V. Debierre, I. Goessens, E. Brainis, and T. Durt, Fermi's golden rule beyond the zeno regime, *Phys. Rev. A* **92**, 023825 (2015).
- [43] A. Neuzner, M. Körber, O. Morin, S. Ritter, and G. Rempe, Interference and dynamics of light from a distance-controlled atom pair in an optical cavity, *Nat. Photonics* **10**, 303 (2016).